Supplementary Information for

Structural Basis for GTP-induced Dimerization and Antiviral Function of Guanylate-binding Proteins

Wen Cui[#], Elisabeth Braun[#], Wei Wang[#], Jinhong Tang[#], Yanyan Zheng[#], Benjamin Slater, Na Li, Cheng Chen, Qingxiang Liu, Bin Wang, Xiu Li, Yinkai Duan, Yunjie Xiao, Ruijiao Ti, Dominik Hotter, Xiaoyun Ji, Lei Zhang, Jun Cui, Yong Xiong, Daniel Sauter*, Zefang Wang*, Frank Kirchhoff*, Haitao Yang*.

*corresponding authors
Email: yanght@shanghaitech.edu.cn; frank.kirchhoff@uni-ulm.de; zefangwang@tju.edu.cn; daniel.sauter@med.uni-tuebingen.de

This PDF file includes:

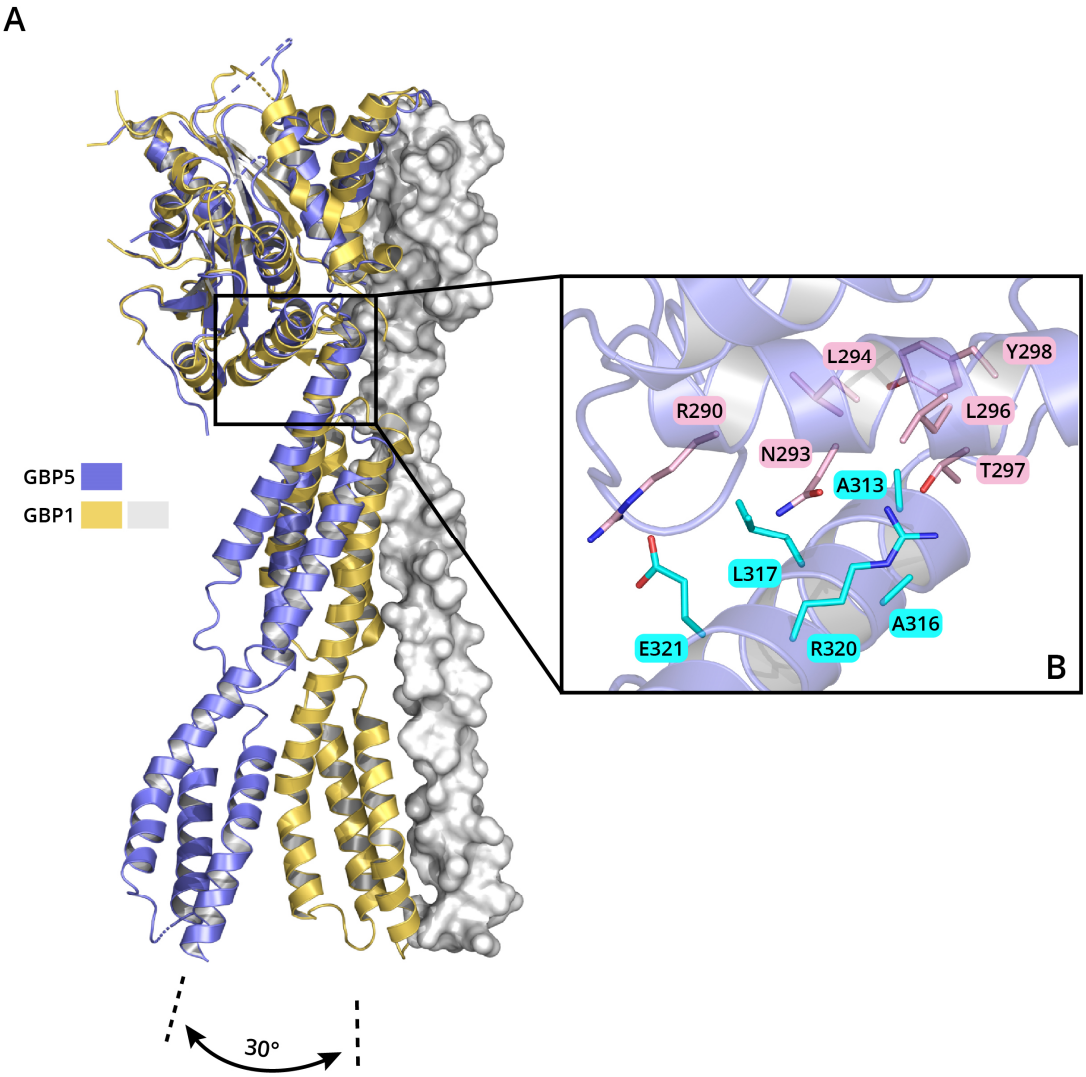

Fig. S1. Structural comparison of the monomeric state of hGBP5$_{1\text{-}486}$ and hGBP1^{FL}.
A) Superposing the structures of hGBP5$_{1\text{-}486}$ (blue) with hGBP1^{FL} (PDB: 1DG3, yellow and grey) based on LG domain shows a swing of MD around the hinge region by 30°. The GED of hGBP1^{FL} is shown in grey surface. The frame indicates region shown in more detail in panel B). B) The interface between LG domain and MD is shown.

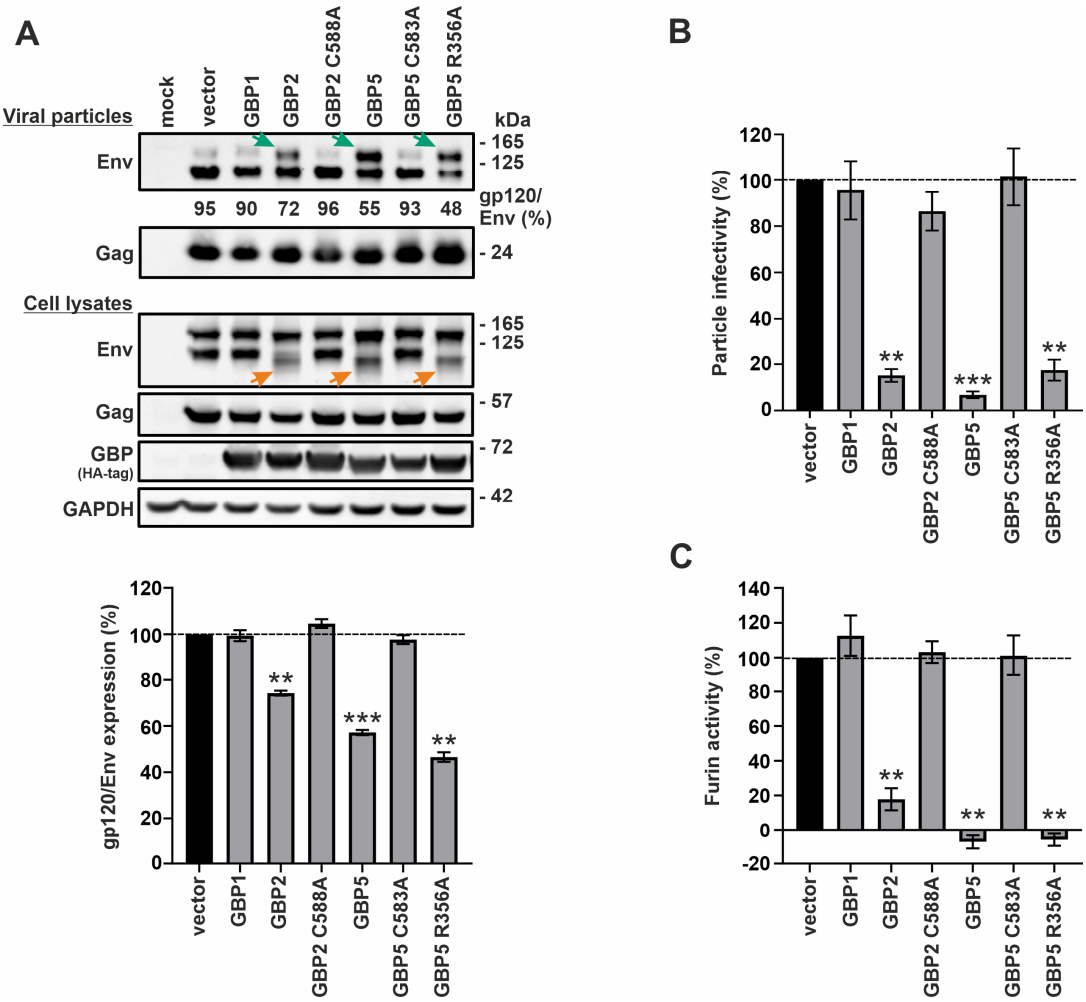

Fig. S2. Mutation R356A does not affect the ability of hGBP5 to reduce furin activity, HIV-1 Env processing or HIV-1 particle infectivity.

A) Western blot analysis of HIV-1 Env and Gag in cells and viral particles when HEK293T cells were co-transfected with an HIV-1 proviral construct and various GBPs (upper panel). The C588A and C583A variants represent previously characterized isoprenylation-deficient mutants of hGBP2 and hGBP5, respectively, that fail to restrict HIV-1 (1). They were included as negative controls. Green arrows indicate an increase of unprocessed Env (gp160) in viral particles. Orange arrows indicate a reduced apparent molecular weight of mature processed Env (gp120) in the presence of some GBP variants. The ratio of mature gp120 to total Env in viral particles was quantified and is shown below a representative western blot as well as the mean of three independent experiments (lower panel). B) Infectious HIV-1 yield in the presence of various GBPs was measured by infection of TZM-bl reporter cells and normalized to the amount of HIV-1 capsid (p24) to calculate particle infectivity. C) Furin activity was measured by Pyr-Arg-Thr-Lys-Arg-7-amino-4-methylcoumarin (AMC) cleavage assay upon co-expression with various GBPs.

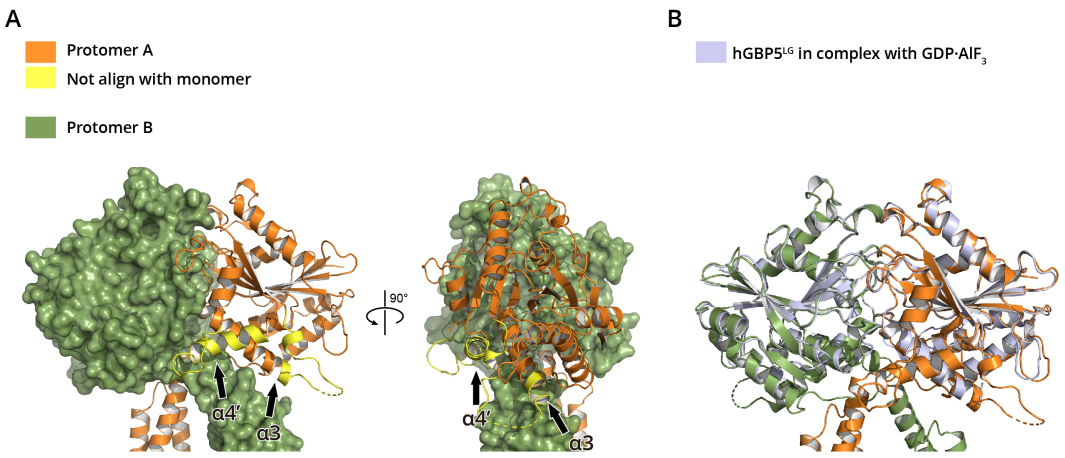

Fig. S3. Structural comparison of the LG domains in hGBP5$_{1\text{-}486}$ dimer and that in hGBP5^{LG} dimer.

A) Two regions at the LG domain which are stabilized by interacting with the MD from the pairing molecule (green) are shown in yellow. B) Superposing the structures of the LG domains in hGBP5$_{1\text{-}486}$ dimer (orange and green) and hGBP5^{LG} dimer (gray) shows that they are highly similar.

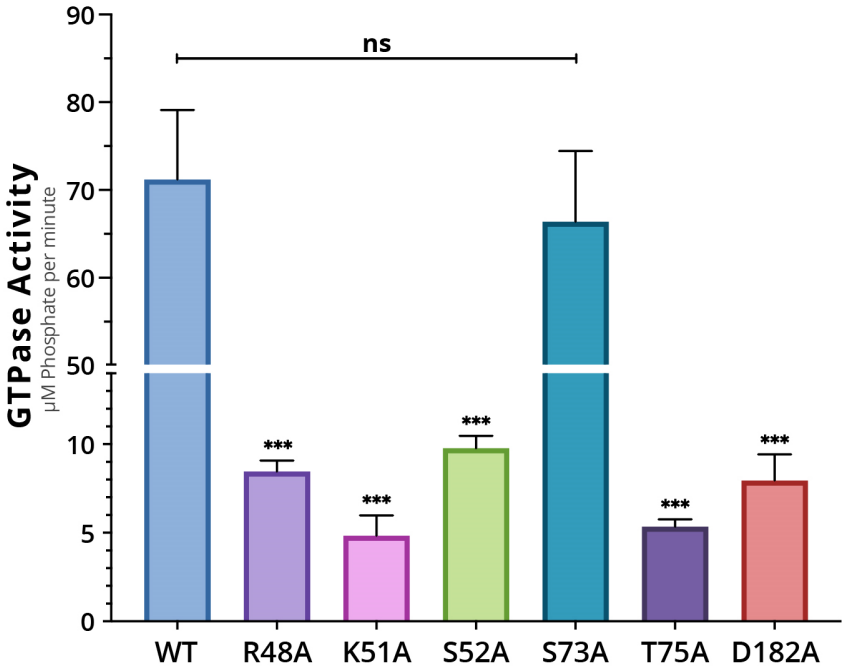

Fig. S4. Effects of mutations in the catalytic core on the GTPase activity of hGBP5.

GTPase activity of WT and mutant hGBP5 were determined as previously described (2). The assays were performed in triplicate, with mean values and standard deviations plotted. Unpaired t-test was performed between WT and each of hGBP5 mutants. "***" indicates $p<0.001$ and "ns" indicates $p>0.05$.

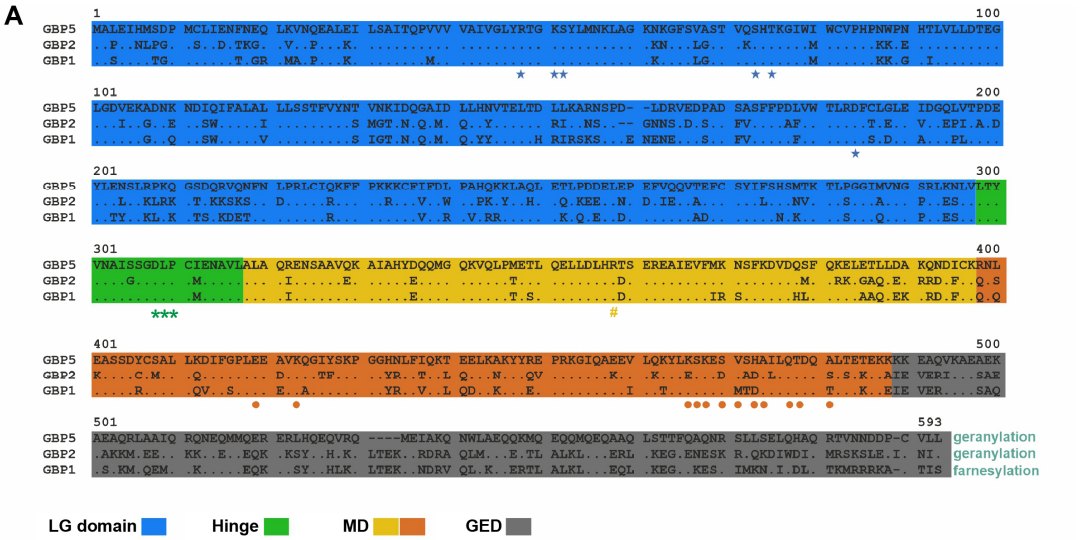
A
GBP5
GBP2
GBP1
geranylation
geranylation
farnesylation
LG domain
Hinge
MD
GED
★ GTPase mutant in GBP5: R48A, K51A, S52A, S73A, T75A, D182A
* Hinge mutant in GBP5/GBP2: D306A/D306P, L307A, P308A
# Crystallization construct mutant in GBP5: R356A
• Dimerization mutant in GBP5: E417A, K421A, K464A, S465A, K466A, S468A, V469A, H471A, A472G, Q475A, T476A, A479G
MDDM-A: E417A, K421A
MDDM-B: K464A, S465A, K466A, S468A, V469A
MDDM-C: H471A, A472G, Q475A, T476A, A479G
MDDM-D: K464A, S465A, K466A
MDDM-E: E417A, K421A, S468A, H471A
MDDM-F: V469A, A472G, Q475A, T476A, A479G

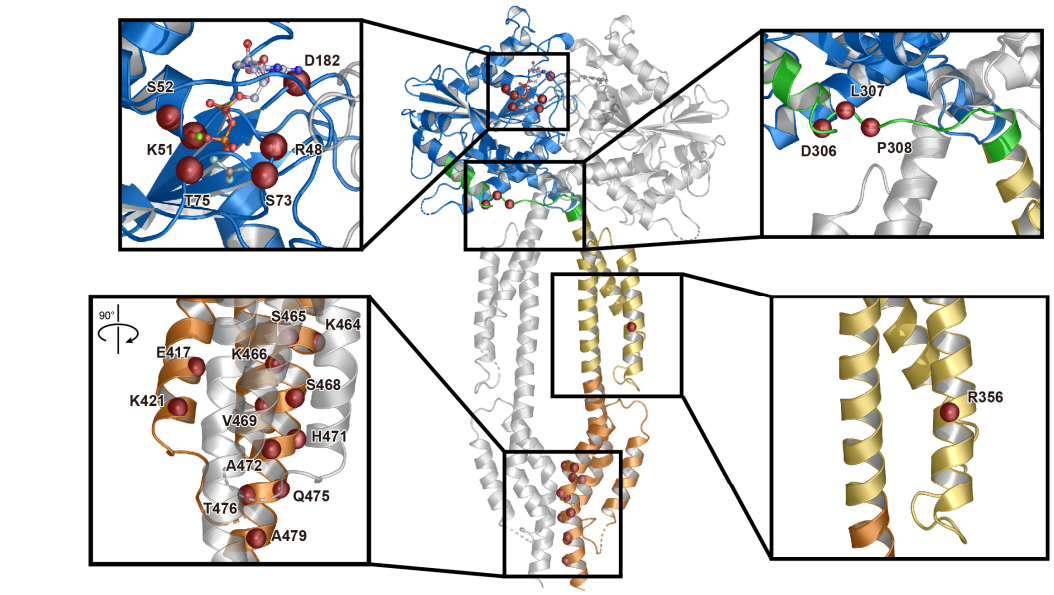
B
D182
S52
K51
R48
T75
S73
L307
D306
P308
90°
S465
K464
E417
K466
S468
K421
V469
H471
A472
T476
Q475
A479
R356

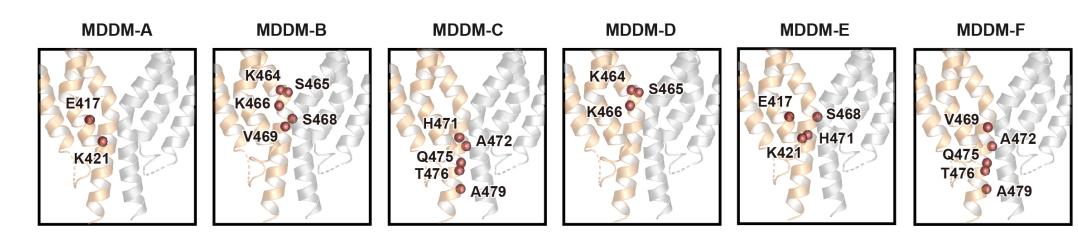
C
MDDM-A
MDDM-B
MDDM-C
MDDM-D
MDDM-E
MDDM-F
E417
K421
K464
S465
K466
S468
V469
H471
A472
Q475
T476
A479
K464
S465
K466
E417
S468
H471
K421
V469
A472
Q475
T476
A479

Fig. S5. Sequence alignment of hGBP1/2/5 with mutations in different domains marked.

A) Protein sequence alignment of hGBP1, hGBP2 and hGBP5. Dashes indicate gaps that were introduced to improve the alignment. LG domain, hinge region, MD and GED are shaded in blue, green, yellow/orange and grey, respectively. Mutants generated and analyzed in this study are highlighted by symbols below the alignment and listed. B) and C) Positions of mutated residues are shown as spheres in the three-dimensional structure of hGBP5.

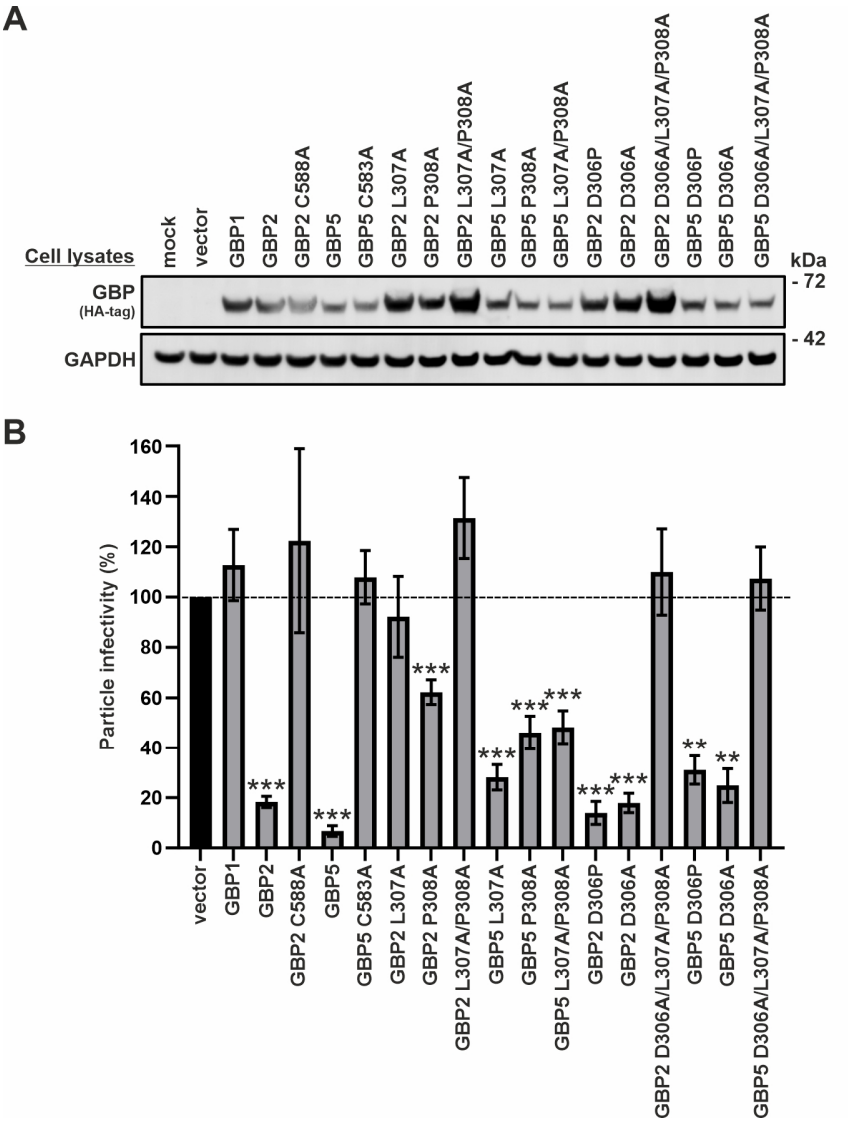

Fig. S6. Mutations in the hinge region reduce the antiviral activity of hGBP2 and hGBP5.

A) Western blot analysis of the expression of all GBPs. HEK293T cells were co-transfected with an HIV-1 proviral construct and various GBPs. The C588A and C583A variants represent previously characterized isoprenylation-deficient mutants of hGBP2 and hGBP5, respectively, that fail to restrict HIV-1. They were included as negative controls. B) Infectious HIV-1 yield in the presence of various GBPs. It was determined by infection of TZM-bl reporter cells and normalized to the amount of HIV-1 capsid (p24) to calculate particle infectivity. Mean values of four to seven independent experiments are shown.

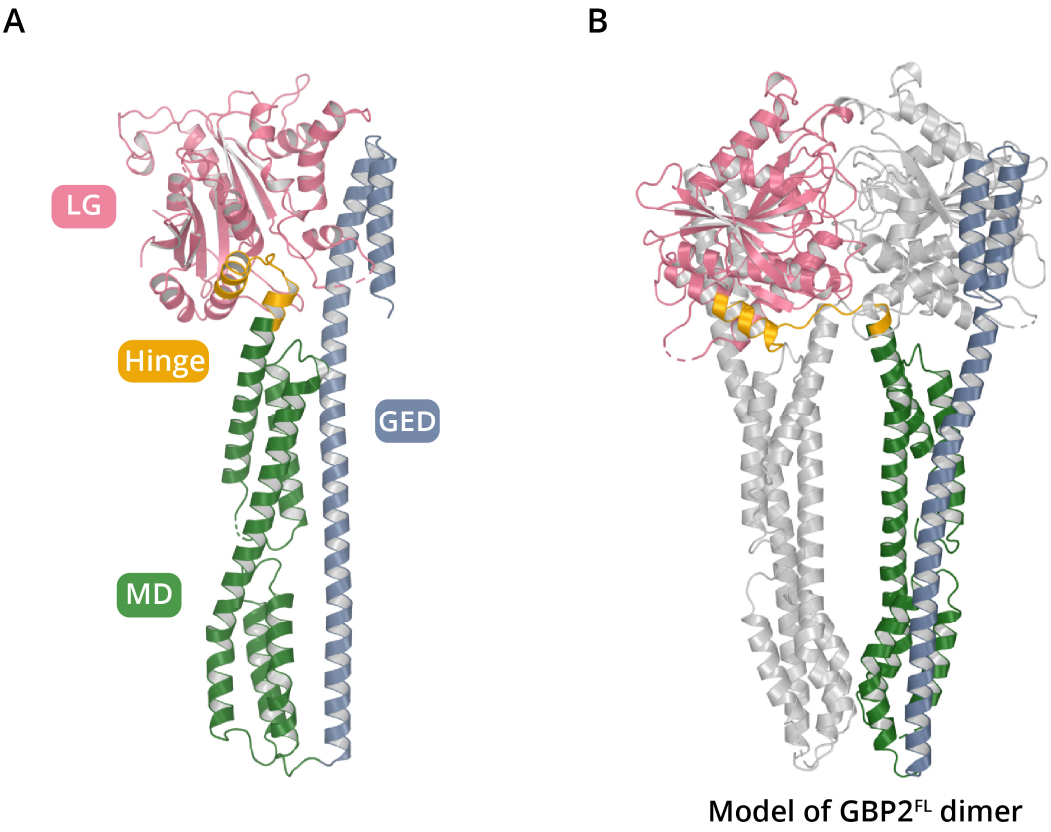

Fig. S7. Crystal Structure of hGBP2^{FL} in nucleotide-free state and a model of hGBP2^{FL} in nucleotide-bound state.

A) The crystal structure of hGBP2^{FL} in its nucleotide-free state. LG domain, hinge region, MD and GED are depicted in pink, orange, green and blue, respectively. B) A model of hGBP2^{FL} in its nucleotide-bound state based on the crystal structure of hGBP5$_{1-486}$ in complex with GDP·AlF$_3$.

Table S1. Data Collection and Refinement Statistics.

	$hGBP5_{1-486}$	$hGBP5_{1-486}$-GDP·AlF_3	$hGBP5^{LG}$-GDP·AlF_3	$hGBP2^{FL}$
Data Collection				
Space group	P22121	P3221	P212121	P212121
Cell Dimensions				
a, b, c (Å)	90.9, 137.3, 203.3	114.3, 114.3, 168.5	65.3, 79.3, 140.2	42.2, 124.2, 355.7
a, b, c (°)	90.0, 90.0, 90.0	90.0, 90.0, 120.0	90.0, 90.0, 90.0	90.0, 90.0, 90.0
Resolution (Å)	50.00-3.00 (3.05-3.00)	50.00-2.50 (2.54-2.50)	50.00-2.28 (2.32-2.28)	50.00-2.60 (2.64-2.60)
Unique reflections	52289(2595)	44229(2199)	33591(1654)	55672(2117)
Completeness (%)	100.0(100.0)	98.7(98.6)	100.0(100.0)	92.4(70.8)
R_{merge}	0.127(1.883)	0.123(1.294)	0.221(1.758)	0.151(1.325)
$I/\sigma I$	18.0(1.1)	16.9(1.5)	10.3(1.0)	10.6(1.3)
$CC_{1/2}$	0.998(0.592)	0.983(0.639)	0.999(0.634)	0.998(0.591)
Redundancy	9.1(9.0)	9.1(7.9)	12.7(12.6)	7.4(7.2)
Refinement				
Resolution (Å)	48.22-3.00	49.48-2.50	47.79-2.28	46.78-2.60
Number of reflections	51718	44127	33531	55160
R_{work}/R_{free}	0.220/0.260	0.211/0.250	0.211/0.258	0.255/0.271
Number of Atoms				
Protein	13005	7370	4033	8838
Ligand/ion	0	66	66	0
Water	0	110	230	37
B-factors				
Protein	107.85	85.30	45.65	71.83
Ligand/ion	-	52.38	39.65	-
Water	-	61.23	47.82	56.98
RMSDs				
Bond lengths (Å)	0.002	0.003	0.009	0.002
Bond angles (°)	0.44	0.64	1.1	0.47
Ramachandran Statistics (%)				
Favored	95.0	96.8	96.6	99.2
Allowed	5.0	3.2	3.4	0.8
Disallowed	0.0	0.0	0.0	0.0

Values in parentheses are for the highest-resolution shell.

Table S2. Primers used to generate pCG IRES BFP expression plasmids.

Construct name	Primer name	Primer sequence (5'-3')
GBP2 wt	GBP2 N-HA XbaI fw	CTTCTAGACCATGTACCCATACGATGTTCCAGATTACGCTGCTCCAGAGATCAACTTGC
	GBP2 MluI rev	GAACGCGTTAGAGTATGTTACATATTGGCTCC
GBP5 wt	GBP5 N-HA XbaI fw	CTTCTAGACCATGTACCCATACGATGTTCCAGATTACGCTGCTTTAGAGATCCACATGTC
	GBP5 MluI rev	CTACGCGTTTAGAGTAAAACACATGGATCATCGTTATTAAC
GBP2 D306P	GBP2 D306P rev	ATGGCATTGACGTAGGTC
	GBP2 D306P fw	CGGCAGTGGGCCTCTACCCTGCA
GBP2 D306A	GBP2 D306A rev	ATGGCATTGACGTAGGTCAGCAC
	GBP2 D306A fw	CGGCAGTGGGGCTCTACCCTGCA
GBP2 L307A	GBP2 L307A rev	CTCCATGCAGGGTGCATCCCCACTGC
	GBP2 L307A fw	GCAGTGGGGATGCACCCTGCATGGAG
GBP2 P308A	GBP2 P308A rev	CGTTCTCCATGCAAGCTAGATCCCCAC
	GBP2 P308A fw	GTGGGGATCTAGCTTGCATGGAGAACG
GBP2 L307A/P308A	GBP2 L307A/P308A rev	CGTTCTCCATGCAAGCTGCATCCCCACTGC
	GBP2 L307A/P308A fw	GCAGTGGGGATGCAGCTTGCATGGAGAACG
GBP2 D306A/L307A/P308A	GBP2 D306A/L307A/P308A rev	GCAGCCCCACTGCCGATGGCATT
	GBP2 D306A/L307A/P308A fw	AGCTTGCATGGAGAACGCAGTC
GBP5 D306P	GBP5 D306P rev	ATGGCATTGACATAGGTC
	GBP5 D306P fw	CAGCAGTGGGCCTCTGCCTTGCATAG
GBP5 D306A	GBP5 D306A rev	ATGGCATTGACATAGGTCAGCAC
	GBP5 D306A fw	CAGCAGTGGGGCTCTGCCTTGCA

Construct name	Primer name	Primer sequence (5'-3')
GBP5 L307A	GBP5 L307A rev	CTCTATGCAAGGCGCATCCCCACTG
	GBP5 L307A fw	CAGTGGGGATGCGCCTTGCATAGAG
GBP5 P308A	GBP5 P308A rev	GCATTCTCTATGCAAGCCAGATCCCCAC
	GBP5 P308A fw	GTGGGGATCTGGCTTGCATAGAGAATGC
GBP5 L307A/P308A	GBP5 L307A/P308A rev	GCATTCTCTATGCAAGCCGCATCCCCACTGC
	GBP5 L307A/P308A fw	GCAGTGGGGATGCGGCTTGCATAGAGAATGC
GBP5 D306A/L307A/P308A	GBP5 D306A/L307A/P308A rev	GCAGCCCCACTGCTGATGGCATT
	GBP5 D306A/L307A/P308A fw	GGCTTGCATAGAGAATGCAGTCC
GBP5 R356A	GBP5 R356A rev	CCCTCTCACTGGTAGCGTGCAGGTCCAGC
	GBP5 R356A fw	GCTGGACCTGCACGCTACCAGTGAGAGGG
GBP5 MDDM	GBP5 MDDM rev	CACTGCTTCTGCCAGAGG
	GBP5 MDDM fw	CCTCTGGCAGAAGCAGTG
	GBP5 MDDM rev	CCAGCACTTGCAGCCTCCGCGGCCGCTAAATATTTC
	GBP5 MDDM fw	GGAGGCTGCAAGTGCTGGAATATTAGCAGCTGACCAGGGTCTCACAGAG
GBP5 MDDM-A	GBP5 MDDM-A rev	GAATAAATTCCCTGGGCCACTGCTTCGGCCAGAGGAC
	GBP5 MDDM-A fw	GTCCTCTGGCCGAAGCAGTGGCCCAGGGAATTTATTC
GBP5 MDDM-B	GBP5 MDDM-B rev	GTAATATTGCATGACTGGCGGCCTCGGCGGCGGCTAAATATTTCTG
	GBP5 MDDM-B fw	CAGAAATATTTAGCCGCCGCCGAGGCCGCCAGTCATGCAATATTAC
GBP5 MDDM-C	GBP5 MDDM-C rev	GTCTCTGTGAGGCCCTGGTCGGCGGCTAATATGCCGGCACTCACAGACTC
	GBP5 MDDM-C fw	GAGTCTGTGAGTGCCGGCATATTAGCCGCCGACCAGGGCCTCACAGAGAC
GBP5 MDDM-D	GBP5 MDDM-D rev	CATGACTCACAGACTCGGCGGCGGCTAAATATTTCTG

Construct name	Primer name	Primer sequence (5'-3')
	GBP5 MDDM-D fw	CAGAAATATTTAGCCGCCG CCGAGTCTGTGAGTCATG
GBP5 MDDM-E	GBP5 MDDM-E rev	GAATAAATTCCCTGGGCCA CTGCTTCGGCCAGAGGAC
	GBP5 MDDM-E fw	GTCCTCTGGCCGAAGCAGT GGCCCAGGGAATTTATTC
	GBP5 MDDM-E rev	CTGTAATATTGCGGCACTC ACGGCCTCCTTGGAC
	GBP5 MDDM-E fw	GTCCAAGGAGGCCGTGAGT GCCGCAATATTACAG
GBP5 MDDM-F	GBP5 MDDM-F rev	GTCTCTGTGAGGCCCTGGT CGGCGGCTAATATGCCATG ACTGGCAGACTCCTTGGAC
	GBP5 MDDM-F fw	GTCCAAGGAGTCTGCCAGT CATGGCATATTAGCCGCCG ACCAGGGCCTCACAGAGAC

SI References

1. E. Braun *et al.*, Guanylate-Binding Proteins 2 and 5 Exert Broad Antiviral Activity by Inhibiting Furin-Mediated Processing of Viral Envelope Proteins. *Cell Rep* **27**, 2092-2104.e2010 (2019).
2. H. Tian *et al.*, Structural basis of Zika virus helicase in recognizing its substrates. *Protein Cell* **7**, 562-570 (2016).